REFERENCES

1. S. B. Thomason, J. C. Mulligan and J. Everhart, The effect of internal solidification on turbulent-flow heat transfer and pressure drop in a horizontal tube, *J. Heat Transfer* **100,** 387–394 (1978).
2. S. B. Thomason and J. C. Mulligan, Experimental observations of flow instability during turbulent flow-freezing in a horizontal tube, *J. Heat Transfer* **102,** 782–784 (1980).
3. P. Sampson and R. D. Gibson, A mathematical model of nozzle blockage by freezing—II. Turbulent flow, *Int. J. Heat Mass Transfer* **25,** 119–126 (1982).
4. M. Epstein and F. B. Cheung, On the prediction of pipe freeze-shut in turbulent flow, *J. Heat Transfer* **104,** 381–384 (1982).
5. R. R. Gilpin, Ice formation in a pipe containing flows in the transition and turbulent regimes, *J. Heat Transfer* **103,** 363–368 (1981).
6. T. Hirata and M. Ishihara, Freeze-off conditions of a pipe containing a flow of water, *Int. J. Heat Mass Transfer* **28,** 331–337 (1985).

Int. J. Heat Mass Transfer. Vol. 30, No. 10, pp. 2205–2209, 1987
Printed in Great Britain

0017–9310/87 $3.00 + 0.00

The transient solidification of weldpools

G. M. Oreper and J. Szekely
Department of Materials Science and Engineering, Massachusetts Institute of Technology, Cambridge, MA 02139, U.S.A.

(*Received* 28 *August* 1986 *and in final form* 22 *April* 1987)

INTRODUCTION

In a recent paper (1984) we developed a formulation and presented computed results describing the transient development of weldpools in spot welds, produced by the TIG (tungsten inert gas) welding process. The physical picture invoked a solid metal block onto which a plasma jet was made to impinge. This plasma jet provided a spatially distributed heat source, causing partial melting of the block. At the same time the molten pool (termed weldpool) would undergo recirculating motion as driven by the combination of:

(a) buoyancy forces;
(b) electromagnetic forces and;
(c) if applicable surface tension forces, due to temperature gradients at the free surface.

In the formulation presented appropriate scaling factors were introduced for time and length, so that the numerical computer results could be usefully generalized.

It was shown that under certain conditions (when the modified Peclet number was large) convection appreciably affected the heat transfer process and hence the shape of the weldpool. While under other conditions (small values of the modified Peclet number) conduction was the dominant mechanism for heat transfer in the weldpool.

In a physical sense the former case corresponded to surface tension driven flows and/or electromagnetically driven flows, caused by a strongly divergent current path in the weldpool, resulting in weldpool shapes that markedly deviated from the idealized shape that one would obtain from the classical point source solutions.

In contrast in the absence of significant convection effects, i.e. for broadly distributed heat sources, the weldpools were essentially ellipsoidal in shape.

The treatment developed in the earlier paper has answered one part of the real physical problem, namely what are the factors that govern the transient growth and shape of a weldpool. However, an equally important part of the weldpool problem has yet to be answered, namely how does convection affect the solidification of the molten region.

In a physical sense this problem may be stated as follows.

Due to the action of the plasma jet and the attendant buoyancy, surface tension and electromagnetically driven flows, a weldpool is generated and is undergoing recirculatory motion. Then the supply of current and hence of thermal energy is discontinued, thus the direction of the melt–solid boundary advancement is reversed and the weldpool is then allowed to solidify.

The question is then to describe this solidification process and also to represent the transient, progressively shrinking weldpool, since the structure of the solidified material, of considerable interest in the assessment of the weldment quality, may be markedly affected by the motion of the liquid, with which it is in contact during the solidification process.

Let us consider a weldpool, which is axisymmetric in shape, such as sketched in Fig. 1. The growth of this weldpool has been initiated at time $-t_0$ and as a result there developed temperature profiles both within the weldpool and in the base metal and a corresponding circulation pattern has also

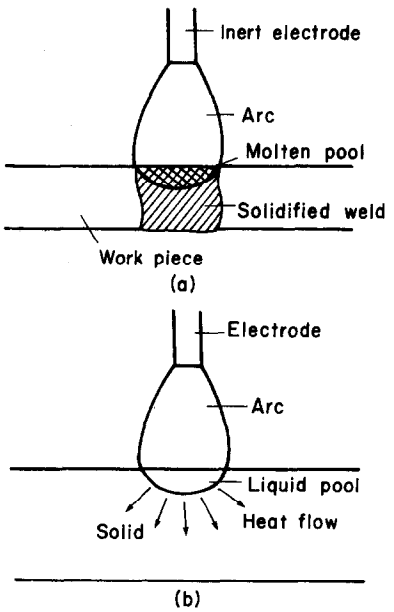

FIG. 1. Schematic sketch of a TIG welding system.

NOMENCLATURE

A aspect ratio
L thickness of metal plate, 3.1×10^{-2} m
R maximum radius of region of calculation, 4.65×10^{-2} m
T temperature [K]
z, r dimensionless coordinates.

Greek symbols
β coefficient of thermal expansion, $10^{-4}\,K^{-1}$
ε emissivity, 0.4
θ dimensionless temperature, $(T-T_0)/(T_l-T_0)$
λ latent heat of fusion, $247\,kJ\,kg^{-1}$
μ viscosity of molten metal, $0.006\,kg\,m^{-1}\,s^{-1}$
ξ vorticity
ρ density of molten and solid metal, $7.2 \times 10^3\,kg\,m^{-3}$
σ Stefan–Boltzmann constant, $5.67 \times 10^{-8}\,W\,m^{-2}\,K^{-4}$
ψ stream function.

Subscripts and superscripts
C_p specific heat of molten and solid metal, $753\,J\,kg^{-1}\,K^{-1}$
K_l thermal conductivity of molten metal, $15.48\,W\,m\,K^{-1}$
K_s thermal conductivity of solid metal, $31.39\,W\,m\,K^{-1}$
L_z weldpool depth
L_R weldpool width
T_0 initial temperature of metal, 300 K
T_l liquidus temperature of metal, 1723 K
T_s solidus temperature of metal, 1523 K
$U_{z,0}, U_{R,0}$ velocity scales.

been established. This represents the initial conditions to our problem.

At time = 0 the heat supply is discontinued and as a result at the melt–solid interface the rate of heat extraction by the solid phase exceeds the rate of heat supply from the molten region and hence the weldpool will solidify. The rate of this solidification may be affected by convective motion within the weldpools, which is likely to diminish with time. As far as weldpool circulation is concerned, motion will persist up to a point because of liquid inertia and the existence of the progressively weaker buoyancy and surface tension forces; the electromagnetic force field will, of course disappear once the plasma arc is extinguished.

The mathematical statement of the problem is identical to that given in the earlier paper, except for the absence of the electromagnetic body force field term in the equation of motion.

Thus the dimensionless form of the vorticity transport equation is given as

$$\frac{r^3}{A^2 Re\,Pr}\frac{1}{k}\frac{L_z^2}{L^2}\frac{\partial \xi}{\partial t} + r^2\left[\frac{\partial}{\partial z}(\xi U_z r) + \frac{\partial}{\partial r}(\xi U_R r)\right] - \frac{1}{Re\,A^2}\frac{\partial}{\partial z}\left(r^3\frac{\partial \xi}{\partial z}\right) - \frac{1}{Re}\frac{\partial}{\partial r}\left(r^3\frac{\partial \xi}{\partial r}\right) - \frac{Gr\,A}{Re^2}\frac{\partial \theta}{\partial r}\frac{T_l - T_0}{\Delta T} = 0 \tag{1}$$

where the Reynolds number

$$Re = \frac{\rho U_{R,0} L_R}{\mu}$$

the Prandtl number

$$Pr = \frac{C_{p,0}\mu}{K_l}$$

and the Grashof number

$$Gr = \frac{g\beta L_R^3 \Delta T \rho^2}{\mu^2}$$

while the differential thermal energy balance equation takes the following form:

$$(St)r\frac{\partial \theta}{\partial t} + Re\frac{L_z}{L}(Pr)k\left[\frac{\partial}{\partial z}\left(\theta\frac{\partial \psi}{\partial z}\right) - \frac{\partial}{\partial r}\left(\theta\frac{\partial \psi}{\partial z}\right)\right] - \frac{1}{C_p}\left[\frac{\partial}{\partial z}\left(kr\frac{\partial \theta}{\partial z}\right) + \frac{\partial}{\partial z}\left(kr\frac{\partial \theta}{\partial r}\right)\right] = 0. \tag{2}$$

The stream function ψ, which appears in the thermal-energy balance equation, may be related to the vorticity by

$$\frac{1}{A^2}\frac{\partial}{\partial z}\left(\frac{1}{r}\frac{\partial \psi}{\partial z}\right) + \frac{\partial}{\partial r}\left(\frac{1}{r}\frac{\partial \psi}{\partial r}\right) + r\xi = 0 \tag{3}$$

where C_p is the dimensionless specific heat, i.e. specific heat/$C_{p,0}$

$$St = \frac{C_{p,0}(T_l - T_0)}{\lambda}$$

is the Stefan number, and λ is the heat of fusion.

In order to allow for the release of the latent heat in the mushy region, the following dimensionless expression was used to represent the specific heat:

$$C_p = \frac{1}{St\Delta\theta_{ls}} + 1$$

where $\Delta\theta_{ls} = \theta_l - \theta_s$ is the temperature range of melting, and θ_s is the solidus temperature of the metal. It should be noted, furthermore, that the thermal conductivity in the mushy zone was assumed to vary linearly between the values for the molten and the solid regions. Equation (2) will be valid for all three regions, with the stream function being zero in the mushy region and in the solid phase.

The length scale used in the integration of both the vorticity-transport equation and the thermal-energy balance equations was the thickness of the plate, while the reference velocity defined for computational purposes was

$$\tilde{U} = \frac{\mu}{\rho L}(\tilde{G}r)^{1/2}$$

where the reference value $\tilde{G}r$ of the Grashof number was evaluated using the plate thickness L as the characteristic length. This procedure was convenient for generating numerical results, because a time-dependent length scale would have introduced unnecessary complications.

The initial conditions have to specify a given weldpool shape; temperature distribution; and circulation pattern in the molten region.

The boundary conditions for equations (1) and (3) take the following form:

$$\frac{\partial \xi}{\partial r} = 0 \quad \text{at} \quad r = 0$$

$$\xi = 0 \quad \text{at} \quad z = 0$$

$$\psi = 0 \quad \text{along all boundaries}$$

which in physical terms specify that the gradient of the vorticity/r has to be zero at the free surface and at the axis of symmetry. The expression used for specifying the vorticity at the melt–solid interface, i.e. at the moving boundary, was given in ref. [1].

The boundary conditions associated with equation (2) take the following form:

$$-\frac{\partial\theta}{\partial z}=\frac{L\varepsilon\sigma T^4}{K_e(T_e-T_0)} \quad \text{at} \quad z=0$$

$$\frac{\partial\theta}{\partial z}=0 \quad \text{at} \quad z=1$$

$$\frac{\partial\theta}{\partial r}=0 \quad \text{at} \quad r=0$$

$$\theta=0 \quad \text{at} \quad r=\frac{R}{L}$$

where T is the absolute temperature (K), ε the emissivity, and σ the Stefan–Boltzmann constant.

When there is a surface-tension gradient at the free surface, caused by the temperature dependence of the interfacial tension, the boundary condition for vorticity has to take the following form:

$$\xi=\frac{M}{Re}\frac{1}{r}\frac{\partial\theta}{\partial r} \quad \text{at} \quad z=0$$

where

$$M=\frac{\rho L_z\Delta T\dfrac{\partial\gamma}{\partial T}}{\mu^2}$$

is the surface-tension parameter and γ the interfacial tension. The quantity M may also be regarded as a surface-tension Reynolds number.

The method of solution to be employed is again identical to that used in the previous article.

COMPUTED RESULTS

Before showing some typical computed results, it is important to consider order of magnitude analyses which may be brought to bear on the principal issues that have to be addressed.

(1) How rapidly will the weldpool diminish once the plasma arc has been extinguished?

(2) What will be the effect of this circulation on the rate at which the molten region solidifies?

The following general characteristic may apply: weldpool circulation will affect the heat transfer process in the weldpool when the modified Peclet number

$$Pe=\frac{U_{R,0}L_RC_{p0}L_z}{Lk_s} \tag{4}$$

is larger than unity.

The decay of the velocity field will be influenced by the following factors:

(a) inertia;
(b) buoyancy;
(c) surface tension and;
(d) viscous forces.

These, in turn, will of course be affected by the system geometry and by the property values of the material.

Circulation will be maintained due to inertia and the time scale associated with the corresponding decay is given by

$$\tau_i=\frac{L^2\rho}{\mu}\sim 10\text{ s}. \tag{5}$$

Circulation will be maintained due to buoyancy forces and here the velocity may be scaled as

$$U\sim\frac{g\beta\nabla TL_z^3\rho}{\mu L_R} \quad \text{when} \quad ReA^2\ll 1$$

or

$$U\sim(gL_z\beta\nabla T)^{1/2} \quad \text{when} \quad ReA^2>1 \tag{6}$$

where $A=L_z/L_R$ and the time dependence is introduced implicitly through the time dependence of T and of L. Furthermore, circulation will be maintained due to surface tension forces and here the velocity may be scaled as

$$U_{R,0}\sim\frac{\partial\gamma}{\partial T}\frac{\Delta TA}{\mu} \quad \text{for} \quad ReA^2\ll 1$$

$$U_{R,0}\sim\left[\frac{\left(\dfrac{\partial\gamma}{\partial T}\right)^2(\Delta T)^2}{\rho\mu L_R}\right]^{1/3} \quad \text{when} \quad ReA^2>1. \tag{7}$$

It should be stressed that the *length scale*, which will obviously diminish as the weldpool collapses is a *key factor* in all these expressions.

The time scale for solidification, t_s is given by

$$t_s\sim\frac{L_z^2C_{p0}\rho}{k_sSt}$$

for the conditions considered here

$$t_s\simeq 0.5\text{ s}. \tag{8}$$

The important conclusions that emerge from these considerations are summarized below.

(1) For the weldpool conditions considered here the time scale for solidification is much shorter than the corresponding values for the inertial decay of the velocity field. This finding has the following important consequences.

(2) For most of the period of collapse of the weldpool, solidification will take place from a circulating, rather than a stagnant, weldpool; this may have important implications regarding the structure and properties (impurity distribution) of the weldments produced.

(3) The velocity will decay as the weldpool collapses, but this will be due to the rapid diminution of the length scale and to the decay in ΔT for surface tension driven flows, rather than to viscosity damping.

(4) At least in the initial stages of the weldpool collapse, convection should play an important role in affecting the heat transfer when the Peclet number is large. Such a behavior is to be expected for strong surface tension driven flows.

In the following we shall present a limited number of computed results illustrating this general behavior.

The input parameters used in these calculations are summarized in Table 1. In essence these correspond to a 'normal mode' of operation with a positive value of the surface tension parameter.

Figure 2 shows the computed velocity field 0.02 s after the current supply has been turned off. The strong counterclockwise circulation pattern is readily evident. Figure 3

Table 1. The parameters used to characterize the heat flux and electric current distribution on the surface: $q=q_0\exp(-\alpha_q r^2)$; $j=j_0\exp(-\alpha_j r^2)$

Parameter	Normal mode
q_0	2.2×10^7 W m^{-2}
α_q	3.18×10^4 m^{-2}
j_0	1.9×10^6 A m^{-2}
α_j	1.3×10^2 m^{-1}

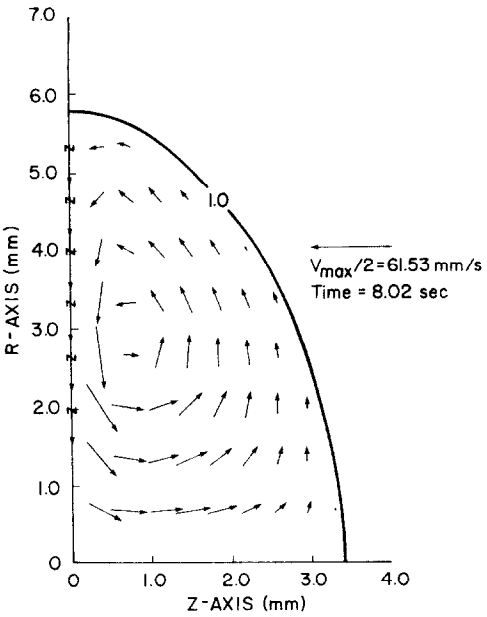

FIG. 2. The computed velocity field for the normal mode of operating, 0.02 s into the solidification period, 8.02 s into the whole cycle.

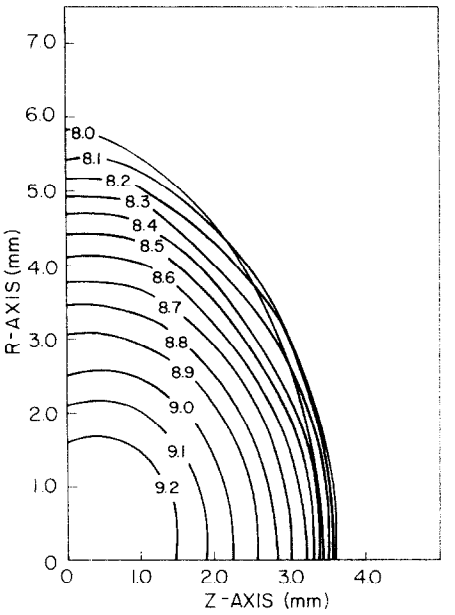

FIG. 4. The computed melt–solid boundary with time as a parameter.

shows the same velocity plot after the passage of 0.5 s into the solidification period. It is seen that the same circulation pattern has been retained, but that the characteristic velocity has now been significantly reduced.

Figure 4 shows the computed solidification patterns, illustrating the gradual collapse of the weldpool.

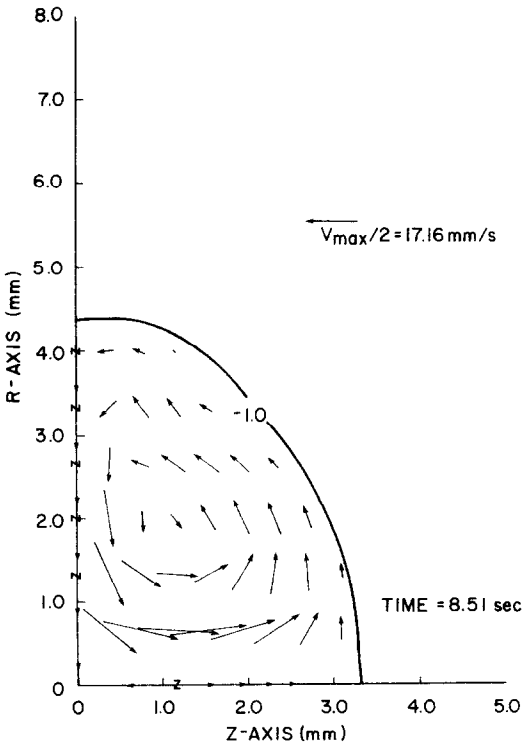

FIG. 3. The computed velocity profiles for the normal mode of operation, 0.5 s into the solidification period.

It is of interest to note that in the very initial stages the weldpool actually expanded at the axis, while it was collapsing at the outer edges.

This finding clearly supports the contention that convection may play an important role in determining the shape of the collapsing weldpool. Finally, Fig. 5 shows the time dependence of the maximum velocity in the weldpool, indicating the quite rapid decay.

It should be noted that Fig. 5 depicts the variation of the maximum velocity during the whole welding cycle, so that time is counted from the initiation of the welding process. This was done in order to provide a perspective regarding the growth and decay of the velocity field.

On commenting on the shape of this curve, we should note that this represents the effect of several conflicting factors. The initial increase in the velocity is due to the corresponding increase in the length scale. The moderate decrease from a maximum is attributable to the fact that a further increase in the pool diameter will reduce the free surface temperature gradient, which is the driving force for the surface tension driven flow. The rapid decay experienced upon the cessation of the heat supply has been discussed earlier; this is due to the combined effect of reducing both the length scale and diminishing the temperature gradient at the free surface.

DISCUSSION

In discussing these results, it is of interest to compare the results of the numerical computation with the order of magnitude predictions that have been developed

$$t_s \simeq 0.5\ \text{s} \tag{9}$$

which compares reasonably well with the computed values of about 1 s.

The time scale for the inertial decay of the velocity has been estimated as

$$\tau_i \sim 10\ \text{s} \tag{10}$$

which is indeed an order of magnitude larger than the solidification time, in clear agreement with the computed results.

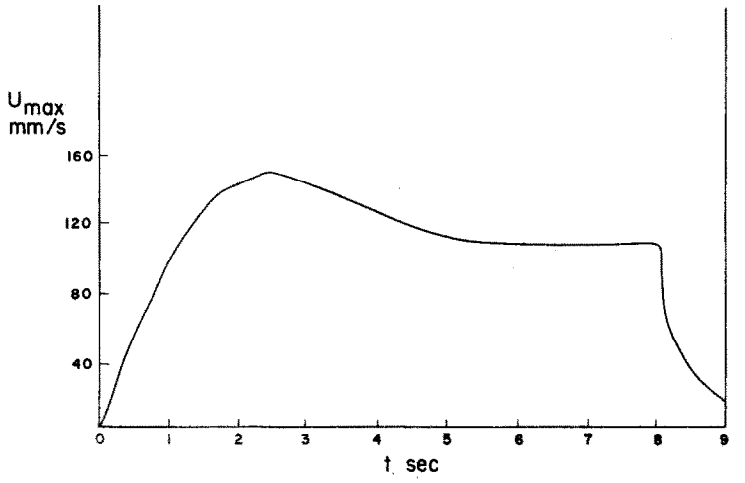

FIG. 5. The computed maximum value of the velocity as a function of time.

The important consequence of this finding is that the velocity field will die out due to the collapse of the weldpool (i.e. the diminution of the length scale) rather than due to viscous damping.

It follows that a good fraction of the solidification will take place from a circulating weldpool.

CONCLUDING REMARKS

A formulation has been developed to represent heat transfer and fluid flow phenomena in the solidification of weldpools, upon the discontinuation of the current supply.

Under these conditions the initial state of the system corresponds to a circulating weldpool, where the liquid motion is driven by the combination of electromagnetic, buoyancy and surface tension forces.

These problems are of considerable practical interest because the way in which the weldpool solidifies may have a marked effect on the structure and properties of the weldments produced.

The order of magnitude analysis has shown that the time scale for solidification is much shorter than the time scale for the inertial decay of the velocity field thus solidification will take place from a circulating melt. Furthermore, in many circumstances the Peclet number is large enough so that convection will have an effect in determining the solidification rate, at least in the initial stages.

The computed results presented in the paper support these conclusions.

Acknowledgments—The authors wish to thank the Office of Naval Research for support under Grant N00014-84-K-0427.

REFERENCE

1. G. M. Oreper and J. Szekely, Heat and fluid flow phenomena in weldpools, *J. Fluid Mech.* **147**, 53–79 (1984).